Available online at www.sciencedirect.com
SCIENCE DIRECT®
Journal of Chromatography A, 1040 (2004) 33–43
JOURNAL OF CHROMATOGRAPHY A
www.elsevier.com/locate/chroma

Extra-column dispersion of macromolecular solutes in aqueous-phase size-exclusion chromatography

G. Grznárová [a], M. Polakovič [a,*], P. Ačai [a], T. Görner [b]

[a] *Department of Chemical and Biochemical Engineering, Faculty of Chemical and Food Technology, Slovak University of Technology, Radlinského 9, 812 37 Bratislava, Slovak Republic*
[b] *Laboratoire Environnement et Minéralurgie, Ecole Nationale Supérieure de Géologie, UMR 7569 Institut National Polytechnique de Lorraine & CNRS, 15, av. du Charmois, BP 40, 54501 Vandoeuvre-lès-Nancy Cedex, France*

Received 24 November 2003; received in revised form 29 March 2004; accepted 30 March 2004

Abstract

A set of dextran standards was used to study the extra-column dispersion in conventional chromatographic equipment at a broad range of molecular weights, different mobile phase flow rates and connecting tube lengths and diameters. All known correlations for the tube dispersion at laminar flow, including those for short tubes, overestimated the values of the variance of the outlet concentration signal. The difference increased with the solute molecular weight and the flow rate. It was assumed that the discrepancy was due to the effect of natural convection invoked by the density differences of the injected dextran solutions and water. A suitable approximation of the relative band spreading was suggested in a form of a power function of the Reynolds and Schmidt numbers. A significant decrease of the dispersion was observed when the chromatography tubing was coiled into a circle. This decrease was successfully predicted combining the existing correlations for long coiled tubes and short straight tubes.

Keywords: Extra-column dispersion; Band broadening; Tube dispersion; Non-ideal injection pulse; Dextran

1. Introduction

The phenomenon of solute dispersion in connecting tubing and auxiliary devices such as injection valves and detectors has been of considerable interest for the optimisation of the design of analytical equipment [1–6]. The quantification of the extra-column dispersion can be of importance also for a correct estimation of molecular weight distribution in size-exclusion chromatography or for the dynamic modelling of chromatographic separations.

The experimental investigation of spreading of injected solute pulse in different parts of chromatographic systems, where the major role played the connecting tubing, has been a subject of numerous studies in the field of liquid chromatography [5,7–18]. The fundamentals of the theory of solute dispersion in tubes of circular cross-section were laid down by Taylor for both laminar [19] and turbulent flows [20]. He derived and experimentally verified a simple equation suitable for the calculation of the axial dispersion coefficient that characterized a symmetrical spread of solute around the central point travelling with the mean flow velocity along the tube. Aris extended the Taylor equation for the cases where the molecular diffusion in the axial direction could not be neglected [21]. The regions of the validity of the Taylor–Aris equation and utilization of the concept of axial dispersion were analyzed in several publications [22–24].

Aris also proved that the solute concentration tended to have a form of normal distribution [21]. Levenspiel derived a simple relationship between the variance of the concentration response function and the axial dispersion coefficient [25]. This relationship combined with the original Taylor equation has often been applied for the estimation of the extra-column dispersion in connecting tubing [11,12,14,16,17,26–28].

The most significant limitation of the Taylor–Aris equation is that it can only be applied to longer times (or tubes) when the molecular diffusion extinguished the radial concentration profiles. Although some analytical equations for

* Corresponding author. Tel.: +421-2-59325920; fax: +421-2-52496743.
E-mail address: milan.polakovic@stuba.sk (M. Polakovič).

0021-9673/$ – see front matter © 2004 Elsevier B.V. All rights reserved.
doi:10.1016/j.chroma.2004.03.066

short times were presented in a later period [29,30], the problem was mostly treated by the numerical solution of the characteristic equation (Eq. (1)) [23,24,31–35]. Based on the numerical simulations, simple empirical equations were suggested for a correlation of dispersion in short tubes [24,31,36], which were also verified experimentally by the same authors [31,36]. Other simple empirical equations were designed directly from experimental data [3,23].

Several other phenomena pertinent to the dispersion in short tubes that were studied theoretically and/or experimentally include: the dispersion of rectangular pulse [36,37], occurrence of double peaks [24,31,36,37], additivity of the variances of connected tubes [31,33] and analysis of natural convection due the density differences between the injected and displacing fluids [38–40].

Several studies have demonstrated that the coiling of a tube into a helix decreased the dispersion compared to a straight tube of the same length. The decrease dependended on the flow character, tube curvature and solute size [3,13,31,41,42]. The effect of these factors is included in a characteristic criterion, the product of the Dean and Schmidt numbers (see Section 2). With the increase of this product above a critical value, it is first observed a secondary flow, then a flow divided into two equal parallel halves is developed and finally the formation of a linear velocity profile occurs accompanied by a dramatic (more than 100 times) decrease of the variance compared to the straight tube.

The bulk of the dispersion studies was carried out with low-molecular solutes. The publication of Ouano and Biesenberger was one of the very few where the short-tube dispersion of a macromolecular solute was treated [43]. Besides observing double peaks at certain conditions, they found that the mean residence times and variances of different polystyrenes were reduced compared to those of low-molecular solutes. They explained it by the formation of a virtual two-phase flow due to the formation of polymer clusters.

Low values of diffusion coefficients of macromolecular solutes significantly influence their spread in the flowing stream of liquid. The extra-column dispersion is thus a significant phenomenon in size-exclusion chromatography either in standard or inverse mode [28,44]. Dextrans, which provide a homologous set of polymers in a broad range of molecular weights, are the most common polymer standards in aqueous-phase chromatography. The objective of this study was to investigate the dextran dispersion in chromatography tubing in a broad range of conditions, which included besides the different molecular weight of dextrans, the variation of volumetric flow rate, length and diameter of the measuring tube and injected volume.

2. Theory

The analysis of dispersion of injected solute at laminar flow in the tubes of circular cross-section is based on a general mass balance equation,

$$\frac{\partial c_s}{\partial t} + u_0\left(1 - \frac{r^2}{R^2}\right)\frac{\partial c_s}{\partial x} = D\left(\frac{\partial^2 c_s}{\partial x^2} + \frac{\partial^2 c_s}{\partial r^2} + \frac{1}{r}\frac{\partial c_s}{\partial r}\right) \quad (1)$$

where c_s is the solute concentration; D the diffusion coefficient; R the tube radius; t the time; u_0 the tube axis flow velocity; r and x the radial and axial co-ordinates, respectively. The diffusion coefficient is typically considered to be constant which may be far from the reality in the case of macromolecular solutes even in dilute solutions (see Section 3.1). The most common simplification of Eq. (1) is achieved through the assumption that the molecular diffusion in the radial direction can fully eliminate the concentration gradients created by convection. The two-dimensional equation is then transformed into the following one-dimensional one,

$$\frac{\partial c_s}{\partial t} + u\frac{\partial c_s}{\partial x} = D_L\frac{\partial^2 c_s}{\partial x^2} \quad (2)$$

In Eq. (2), u is the mean flow velocity and D_L denotes the axial dispersion coefficient that is defined by Eq. (3) [21].

$$D_L = D + \frac{u^2 d^2}{192D} \quad (3)$$

where d is the tube diameter. In liquid systems, the value of D is almost always much smaller than the second term on the right-hand side of Eq. (3) since the influence of molecular diffusion in the axial co-ordinate is negligible compared to that of convective flow.

The disappearance of radial concentration profiles is achieved only after a sufficiently long time after the injection of solute [19]. This means if the solute concentration is measured locally in a certain distance from the injection this should be sufficiently long so that Eq. (2) could be valid [19,25]. The best quantity for the assessment of the validity of Eq. (2) is the dimensionless time:

$$\tau = \frac{Dt_r}{R^2} \quad (4)$$

where t_r is the mean residence time defined as the ratio of the tube volume and the volumetric flow rate of mobile phase. Ananthakrishnan et al. [23] showed that for solutes with the product of Reynolds number ($Re = du\rho/\mu$; where ρ is the density and μ the dynamic viscosity) and Schmidt number ($Sc = \mu/\rho D$) higher than 200 (valid for most mobile phases in liquid chromatography), τ should be higher than 1.6. In fact, the value of the critical time in the mentioned article was 0.8 but this was related to the axis not the mean velocity.

For a solute injection approximated by the Dirac δ-function, analytical solutions of Eq. (2) were obtained [19,25]. The following simple expression was derived for the variance σ^2 of the normalized (to the amount of solute per tube volume) outlet concentration [25]:

$$\sigma^2 = t_r^2\left[8\left(\frac{D_L}{uL}\right)^2 + \frac{2D_L}{uL}\right] = t_r^2\left[\frac{8}{Pe^2} + \frac{2}{Pe}\right] \quad (5)$$

L denotes here the tube length and Pe the axial Péclet number which is a commonly used measure of axial dispersion in chromatography and reaction engineering [45,46]. The first term in the squared brackets of Eq. (5) becomes negligible for long tubes ($Pe > 200$ which corresponds to $\tau > 6.25$) and the normalized concentration function gets the form of the Gaussian curve [25]. If the axial dispersion coefficient is then expressed from the simplified form of Eq. (3), an equation is obtained which is commonly referred to as the Taylor equation:

$$\frac{\sigma^2}{t_r^2} = \frac{ud^2}{96LD} \tag{6}$$

It is well known that the variance calculated from the Taylor equation is the same as the one obtained from the theoretical plate theory where the number of theoretical plates $n = Pe/2$.

Although Eq. (6) has commonly been used for the estimation of extra-column dispersion in chromatography [11,12,14,16,17,26–28], its use may be problematic due to short lengths of chromatographic connecting tubes. Two empirical equations suitable for the description of dispersion in short tubes were adopted from literature in this study. Atwood and Golay suggested an equation suitable for the elution curves of the slice content type (A detector signal proportional to the solute content in the whole tube cross-section) [31]. It had a form:

$$\frac{\sigma^2}{t_r^2} = \frac{(1 + 8/n_a)^{-2/7}}{n_a}, \quad n_a \geq 0.01 \tag{7}$$

where

$$n_a = \frac{96LD}{ud^2} \tag{8}$$

is the apparent number of theoretical plates calculated from the Taylor equation. An equation suggested by Kolev [3] for $\tau < 0.6$ was rearranged into the following form:

$$\frac{\sigma^2}{t_r^2} = 1.314 n_a \tau^{0.455} \tag{9}$$

The characteristic dimensionless parameter, the Dean number De, is introduced for the assessment of the decrease of dispersion in coiled tubes,

$$De = Re\sqrt{\varphi} \tag{10}$$

where φ is the ratio of the diameters of tube and coil. The product of Schmidt and squared Dean numbers defines several regions of the effect of centrifugal forces on the character of solute dispersion. Since the values of De^2Sc in our study varied from 10^3 to 5×10^5, we used a relationship presented by Leclerc et al. [47]:

$$\phi = 0.75 Re^{-1/3} \tag{11}$$

where ϕ is the ratio of the variances in coiled and straight (calculated from the Taylor equation) tubes of the same length and diameter.

3. Experimental

3.1. Solutes and their physical properties

A homologous set of dextrans (Fluka Chemika AG, Buchs, Switzerland and Sigma, St. Louis, MO, USA) with approximate relative molecular weights 1500; 6000; 9300; 17,500; 40,000; 60,000; 70,000; 110,000; 200,000; 500,000; and 2,000,000 were used as macromolecular solutes. The polydispersity index of individual solutes varied from 1.4 to 2.3. KNO_3 of analytical grade was used in the experiments with a low-molecular solute. Re-distilled water was used for the preparation of injection samples in which the solute concentration was always 10 g/l.

The dynamic viscosity of dextran solutions, μ, was calculated from the following relationship:

$$\mu = [\eta] c \mu_w + \mu_w \tag{12}$$

where c is the dextran concentration; μ_w the water viscosity; and $[\eta]$ the intrinsic viscosity, which was expressed as the following function of the relative molecular weight M_r [48],

$$[\eta] = 0.243 M_r^{0.42} \tag{13}$$

The dynamic viscosity of KNO_3 solutions was taken to be equal to that of water.

For the prediction of the diffusion coefficients of dextrans at infinite dilution, D_0, the following relationship was applied [49–51],

$$D_0 = k_1 M_r^{k_2} \tag{14}$$

The coefficients $k_1 = 4.78 \times 10^{-9}\ m^2\ s^{-1}$ and $k_2 = -0.4409$ were obtained by fitting 18 experimental values of D_0 selected from different sources [49–56]. The mean error of the fit was $3.8 \times 10^{-12}\ m^2\ s^{-1}$. D_0-values were applied in the theoretical predictions used in the Sections 4.2 and 4.4.

Different forms of the equations expressing the dependence of diffusion coefficients in aqueous solutions, D, on the dextran concentration have been reported [49–51,57]. These equations agreed on a general trend of the increase of D with c and they provided the values which coincided quite well at dextrans with lower molecular weights [49,50]. Somewhat larger discrepancies were found at dextrans with the largest molecular weights but it was difficult to judge on the quality of the data provided by different authors [49,50,57]. The most comprehensive set of data was presented by Lebrun and Junter [50] who approximated them with a straight-line concentration dependence in the form,

$$D = D_0(1 + k_D c) \tag{15}$$

The coefficient k_D was proportional to the molecular weight of solute but it had different values for lower and higher molecular-weight intervals (Table 1). If the values of D for 1% solutions of dextrans were calculated, their relative increase compared to D_0 was from 10 to 350%. The values of D were used as the reference values for the calculation of Sc in the Section 4.3.

Table 1
Parameters of the dependence of the coefficient k_D in Eq. (15) on the relative molecular weight in the form $k_D = A + BM_r$ [50]

	A	B
$M_r < 10^5$	11.17	7.65×10^{-4}
$M_r > 10^5$	62.58	9.59×10^{-5}

The diffusion coefficient of KNO_3 at infinite dilution at 25 °C was 1.93×10^{-9} m^2 s^{-1} [58]. The influence of concentration was neglected in this case.

3.2. Injection experiments

All experiments with dextrans were performed in a standard chromatographic system without column consisting of a HPLC pump (ECOM, Praha, Czech Republic) with two heads, 6-port injection valve and differential refractometer both from Knauer (Berlin, Germany). The capillary inside the detector connecting the inlet with the detector cell was 0.9 m long with an inner diameter of 0.25 mm. The detector cell had the diameter of 1 mm and it was 1.15 cm long with the volume of 9 μl. These components were connected with teflon capillaries with the inner diameters of 0.5 or 0.25 mm and the outer diameter of 1/16 of inch.

The mobile phase was re-distilled water. Experiments were performed at a varying flow velocity, injected sample volume and length of measuring tube. Data were collected using the chromatographic station CSW (DataApex Ltd, Praha, Czech Republic). Each injection was repeated three times and the mean values from these replicates were used for presentation and further correlations.

In the first set of experiments, the solutions of dextrans of different molecular weight were injected into systems with the measurig tube lengths L_t equal to 0.35, 0.59, and 2 m with the inner diameter d_t of 0.5×10^{-3} m or with $d_t = 0.25 \times 10^{-3}$ m and $L_t = 1.28$ m. The injection loop tube was 0.293 m long and had a diameter of 0.25×10^{-3} m which corresponded to the volume of 14.4 μl. In the second set of experiments, a solution of single dextran with the molecular weight of 70,000 was used. The measuring tube with $d_t = 0.25 \times 10^{-3}$ m had a length of 1.28 m whereas the tube lengths of 0.35, 0.59, 2, and 4 m were used at $d_t = 0.5 \times 10^{-3}$ m. The injection loop was made of the tube with the diameter of 0.25×10^{-3} m and appropriate lengths which resulted in the injected volumes of 14.4, 50, and 188 μl, respectively.

The volumetric flow rate of mobile phase varied from 0.1 to 1.5 ml min^{-1}, which resulted in the values of the Reynolds number from 2 to 60 in measuring tubes with $d_t = 0.5 \times 10^{-3}$ m or from 8.5 to 127.3 in tube with $d_t = 0.25 \times 10^{-3}$ m.

The experiments with KNO_3 ($M_r = 101$) were performed using the HP 1081B Liquid Chromatograph equipped with UV-Vis HP 1040A Detection System (2 nm resolution) and a computer data acquisition system HP ChemStation (Hewlet Packard, Palo Alto, CA). Two measuring tubes were used to connect the injection valve with the detector; the first one was 0.792 m long with $d_t = 0.5 \times 10^{-3}$ m and the second one 0.733 m long with $d_t = 0.25 \times 10^{-3}$ m. The capillary inside the detector was 0.7 m long with an inner diameter of 0.3 mm. The volume of the detector cell was 4.5 μl. The flow rates were 0.5, 1 and 1.5 ml min^{-1} and the injected volume of a solute was 20 μl.

3.3. Evaluation of injection measurements

The response signal of the chromatographic system $S(t)$ was used to calculate the residence time distribution function $E(t)$ (Eq. (16)), the mean residence time t_r (Eq. (17)) and the variance σ^2 (Eq. (18)).

$$E(t) = \frac{S(t)}{\int_0^\infty S(t)\,\mathrm{d}t} \tag{16}$$

$$t_r = \int_0^\infty tE(t)\,\mathrm{d}t \tag{17}$$

$$\sigma^2 = \int_0^\infty t^2 E(t)\,\mathrm{d}t - t_r^2 \tag{18}$$

The integration was performed by the chromatographic software CSW version 1.7 (DataApex, Praha, Czech Republic). It was checked that the integral in the denominator of Eq. (16) corresponds to the mass of injected solute calculated from the volume of the injection loop and dextran solution concentration. The mean deviation of the difference of these two values was 1.5% where the positive and negative values were essentially symetrically distributed. The mean relative errors of t_r, σ^2, and t_r^2/σ^2 obtained from the replicates were 1.6, 4.2, and 5.7%, respectively.

3.4. Theoretical predictions of t_r and σ^2

The experimental system between the sites of solute injection and detection was formed by four parts: the injection loop, measuring tube, detector capillary, and detector flow cell. The following assumptions were made in order to estimate the mean residence time and variance:

1. Both the residence time and variance were considered to be additive and their values were obtained by the summation of the calculated values for each of the four parts.
2. The residence time in each part equalled to the ratio of its volume and the volumetric flow rate of mobile phase, except for the injection loop where a half of its volume was used since the centre of the injected volume in zero time was in the middle of the injection tube.
3. The variances in the measuring tube, detector capillary, and flow cell were expressed from one of the equations presented in the Theory (Eqs. (6), (7), (9), and (11)) using the diffusion coefficients at infinite dilution.
4. The variance in the injection loop, σ_i^2, was calculated assuming the rectangular response function of the width equal to $2t_{r,i}$, where the last quantity is the residence time

in the injection loop. The integration using Eq. (18) gave the following simple relationship,

$$\sigma_i^2 = \frac{t_{r,i}^2}{3} \quad (19)$$

The assumption of the additivity may lead to a certain underestimation of the total system variance since it is valid only if a perfect mixing occurs at the transfer of the fluid between two segments [31].

4. Results and discussion

The laminar-flow dispersion of solutes in tubes of circular cross-section depends on the tube length and diameter, the flow velocity, viscosity and density of bulk mobile phase, and diffusion coefficient of solute. In order to investigate the extra-column dispersion of macromolecular solutes at a broad range of conditions, pulse injection experiments were carried out at two different tube diameters, several measuring tube lengths, flow rates and molecular weights of dextrans.

4.1. Effect of pulse size

Injection loops of different volume were used in order to examine the effect of the relative size of input rectangular pulse. The pulse-to-system volume ratio was changed from about 1.7 to 60% by combining different measuring tubes and injection loops and the solute was the dextran with the relative molecular weight of 70,000. The variances of the measured outlet concentration at individual tubes exhibited a linear relationship both on the total system volume and injected volume (Fig. 1). This corresponded well to the simulation results of Gill and Ananthakrishnan [37] who predicted the independence of the variance of the residence time distribution on the pulse size up to the volume ratio of 40%. Moreover, the extrapolated value of the experimental variance to the zero volume was very close to zero, which confirmed that, other effects, such as disturbances of velocity profiles in the connectors and locations of cross-section changes or detector dynamics, had a negligible influence on the overall extra-column dispersion.

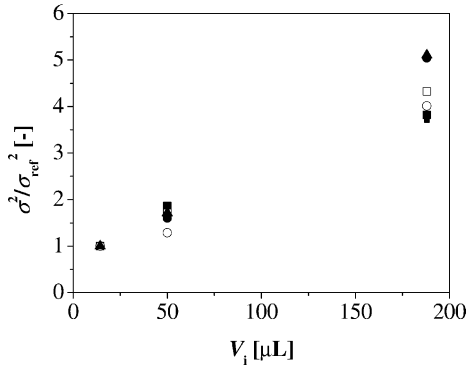

Fig. 1. The variance vs. the injected volume in the system with the capillary 1.28 m long at the following flow rates: (■) 0.1, (□) 0.25, (▲) 0.5, (△) 0.75, (●) 1, and (○) 1.5 ml min^{-1}. At each flow rate, the variances were related to σ_{ref}^2, the variance in the system with the injected volume of 14.4 μl.

The linear relationship of the variance on the injected volume presented in Fig. 1 indicated that the variances of individual parts of chromatographic system were not additive as could be assumed if the variance were proportional to the square-root of the injected volume [27]. From the latter type of relationship in a system with column, Liu et al. were able to make a deconvolution of the variance of the injection device [27]. They found that the proportionality constant between the variance, σ^2, and squared mean residence time in the injection loop, $t_{r,i}^2$, was about twice higher (0.72−0.8) than that one calculated for the rectangular response function (Eq. (19)). When we plotted our experimental results in the form of the dependence of σ^2 on $t_{r,i}^2$, we found that the slope decreased with the injected volume. It went down to about 0.35–0.4 when the injected volume was larger than the volume of residual parts of the system. Obviously, the variance in the injection loop was dominating in this case and only slightly differed from the variance of the rectangular pulse. We therefore preferred to use Eq. (19) for the calculation of the variance of the injection loop. On the other hand, the slope of the mentioned relationship increased at lower injected volumes since a stronger influence of the dispersion in the connecting tubes occured. All further experiments presented below were made with the smallest injection tube of the volume of 14.4 μl. The injected volume was then at maximum 11% of the total system volume. This fraction also represents a maximum possible contribution of the variance of the injection loop to the system variance. Using Eq. (19), this contribution was below 3%. A similar small impact on the dispersion had the detector cell which was at maximum 7% of the system volume. So the main two parts contributing to the dispersion were the measuring tube and thermostatting detector capillary.

4.2. Residence time distribution characteristics—experiments and theory

The experimental residence time distributions had a form close to the normal distribution function only at the lowest molecular weight dextrans when low flow rates and longer tubes were used. The required tube length to achieve the Gaussian function form significantly increased with the flow rate and dextran molecular weight. A simple calculation showed that at the dextran with the relative molecular weight of 2,000,000 and the highest flow rate of 1.5 ml min^{-1}, the required length of the tube with the inner diameter of 0.5 mm would be about 2 km.

Typical shapes of measured concentration signal in short tubes are presented in Fig. 2. At the lower flow rates, the peaks had a character typical for short tubes, with shouldering and signs of double peaks. At the higher flow rates, the peaks were surprisingly sharp. The peaks were

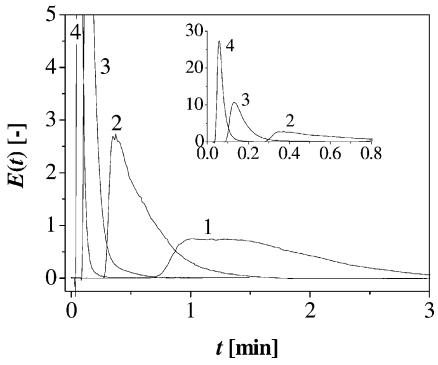

Fig. 2. Residence time distribution function E(t) for the dextran with the relative molecular weight of 70,000 in the measuring tube 0.35 m long with $d_t = 0.5 \times 10^{-3}$ m at different flow rates. (1) $F = 0.1$ ml min^{-1}, (2) $F = 0.25$ ml min^{-1}, (3) $F = 0.75$ ml min^{-1}, and (4) $F = 1.5$ ml min^{-1}.

asymmetrical with a steep onset that occurred at the time very close to the value of 50% of the mean residence time. It means that a significant portion of the solute traveled through the system at the tube axis velocity.

The strong decrease of the relative experimental variance of high-molecular solutes in short tubes with the flow rate is illustrated in Fig. 3. The experimental values, σ^2, were compared to the values calculated using the Taylor equation, σ_T^2 (Eq. (6)). The ratio of σ^2 to σ_T^2 decreased from the values of several tenths at the lowest flow rate of 0.1 ml min^{-1} to several thousandths at the highest flow rates. On the other hand, at comparable residence times of a low-molecular solute, KNO_3, the ratio decreased only to several tenths at the highest flow rate and it was close to 1 at the lower flow rates (Fig. 3). This is not surprising as the dimensionless time τ approached here the critical value of 2 above which the axial dispersion concept is valid (Fig. 4). On the contrary, τ-values of dextrans were much lower than 1 and they were the lower the higher M_r were. Fig. 4 also shows that the experimental variances were approximately in the same range for all dextrans used but the residence times needed to achieve a fully developed axial dispersion flow were much longer at larger dextrans due to their lower diffusivities.

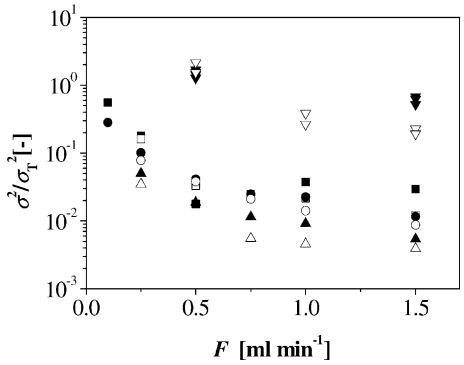

Fig. 3. Effect of flow rate on dispersion of high- and low-molecular solutes, respectively, in short tubes. The experimental variance σ^2 is related to the variance σ_T^2 based on the Taylor equation (Eq. (6)). The presented experiments with high-molecular solutes were made in a system with $L_t = 1.28$ m and $d_t = 0.25 \times 10^{-3}$ m and the results for the following molecular weights of dextrans are plotted: (■) 6000; (□) 17,500; (●) 70,000; (○) 200,000; (▲) 500,000; (△) 2×10^6. The experiments with KNO_3 were conducted in a system with the measuring tube either 0.733 m long with the diameter $d_t = 0.25 \times 10^{-3}$ m (▽) or 0.792 m long with $d_t = 0.5 \times 10^{-3}$ m (▼).

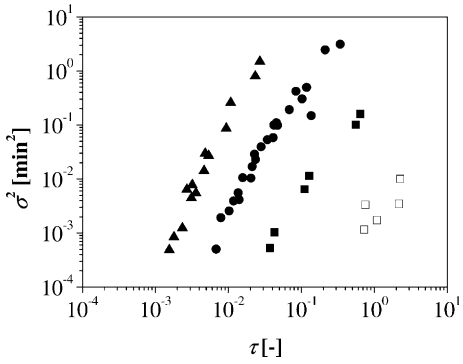

Fig. 4. Experimental variance vs. the dimensionless time. The individual symbols represent solutes with different molecular weights. (■) Dextran ($M_r = 1500$), (●) dextran ($M_r = 70{,}000$), (▲) dextran ($M_r = 2{,}000{,}000$) and (□) KNO_3. The experiments with dextrans were performed in systems with with $d_t = 0.5 \times 10^{-3}$ m and $L_t = 0.35$, 0.59, and 2 m and the range of flow rates 0.1–1.5 ml min^{-1}. The conditions of KNO_3 dispersion measurements were the same as those in Fig. 3.

A relatively small effect of dextran molecular weight on the absolute value of variance is best illustrated in Fig. 5. The variance increased only about twice when the molecular weight increased from 1500 to 2,000,000. On the other hand, about 20-fold increase was predicted for the same range of molecular weights from the Taylor equation. Fig. 5 moreover shows the comparison of the experimental data with the predictions obtained from the equations designed for the region of $\tau < 2$. It is however necessary to emphasize that the Atwood–Golay (Eq. (7)) and the Kolev (Eq. (9)) equations were experimentally validated only for $n_a > 1$ or $\tau > 0.05$, respectively. They are more-or-less equivalent only for $n_a >$

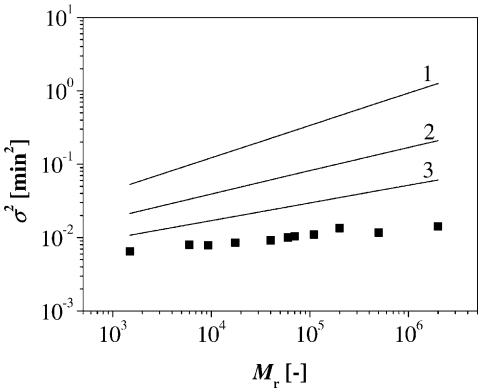

Fig. 5. Effect of dextran molecular weight on dispersion in short tubes. The squares represent the values of variance measured in a system with $L_t = 0.35$ m and $d_t = 0.5 \times 10^{-3}$ m for the flow rate equal to 0.5 ml min^{-1}. The lines represent the variances calculated from different equations: (1) Eq. (5), (2) Eq. (7), and (3) Eq. (9).

3 or $\tau > 0.125$ where the difference in the predicted variance values is less than 20%. At lower values of the dimensionless time, the differences between the two equations grows. The Atwood–Golay equation predicted a much larger variance as demonstrated in Fig. 5 where the τ-values in the measuring tube were in the interval from 1.5×10^{-3} to 2.5×10^{-2}. This equation was obviously not suitable for the description of the experimental data.

The Kolev equation provided a much better estimate of the experimental variance than the two previous equations. At the dextran with the lowest molecular weight, the deviation was less than 50% (Fig. 5). The discrepancies, however, grew with M_r where the estimated variances in short tubes were still several times higher than the experimental ones (Fig. 5). Although the Kolev equation was not experimentally verified for such short relative times as those used in this study, it is useful to discuss the possible sources of the discrepancies between the experimental and predicted values. As it was indicated at the end of the Section 3.4, the convective character of dispersion in a connected short segments of the chromatographic system could lead to that the total variance calculated by the summation of the variances of individual segments could be under estimated but not overestimated as happened here. Moreover, the variances of the measuring tube were by far larger than the variances of other parts so the error of the estimation of the total variance should not be large.

The concentration dependence of viscosity and diffusion coefficient could also play some role. As the values of both quantities increase with the dextran concentration they would have a mutually opposite effects. The viscosity would enhance the dispersion and diffusion coefficient would diminish it. We expect that the overall effect would be a minor one since the injected solution was significantly diluted in all cases and the velocity and concentration profiles would not be modified to such an extent that it would explain the observed discrepancies.

Another factor that could contribute to the observed reduction of the relative variance with the flow rate and molecular weight was the action of natural convection. The natural convection was caused by the density differences (up to 0.3%) between the injected dextran solutions and water. This conclusion qualitatively agrees well with the analysis made by Reejhsinghani et al. [39]. As has been explained by the mentioned authors, the density gradient invokes both axial and radial mixing where the former effect enhances dispersion and the latter one diminishes it. At certain conditions (characterized by the values of the product *Re* and *Sc*), the two sources of natural convection eliminated each other in the effect on the dispersion of injected solution. Fig. 5 shows that the elimination of natural convection effects essentially happened at the dextran with $M_r = 1500$.

Another well-documented observation in thin tubes was that the effect of natural convection on dispersion was observable only at short residence times ($\tau < 2$) [39,43] since the concentration gradients attenuated at longer times.

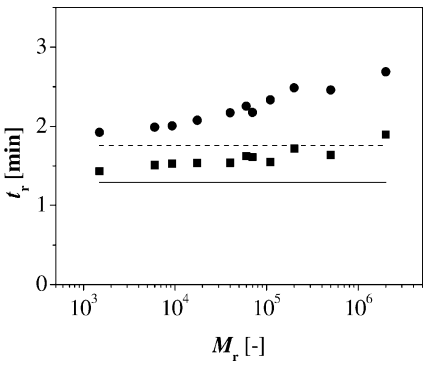

Fig. 6. Mean residence time vs. dextran molecular weight at $F = 0.1\,\mathrm{ml\,min^{-1}}$. The symbols represent the experimental values in a tube with $d_t = 0.5 \times 10^{-3}$ m of different lengths: (■) $L_t = 0.35$ m and (●) $L_t = 0.59$ m. The lines represent the values calculated as the ratio of the system volume and flow rate; — for $L_t = 0.35$ and ---- for $L_t = 0.59$ m.

This complies again very well with our results presented in Fig. 3 where the departure from the axial dispersion model strongly increased at higher flow rates.

Further anomalies that could also have been connected with the effect of natural convection were observed at the experimental values of mean residence time, t_r, evaluated from the response function of the system (Eq. (17)). Fig. 6 illustrates that t_r-values at the lowest flow rate of $0.1\,\mathrm{ml\,min^{-1}}$ increased with the dextran molecular weight approximately in the same proportion at two different tube lengths. Moreover, Table 2 shows that the mean residence time was not inversely related to the flow rate as it would be expected for an ideal longitudinal tube flow. The ratio of the experimental and calculated values of t_r decreased with the increasing flow rate. This conclusion is compatible with the observations made by Ouano and Biesenberger [43] that were attributed to the effect of natural convection without an analysis comparable to the one presented above for the solute dispersion.

Table 2
The mean absolute and relative errors, $\bar{\delta}$ and $\bar{\delta}_r$, respectively, of prediction of t_r at different flow rates and tube lengths

F (ml min^{-1})	L_t (m)	$\bar{\delta}$ (min)	$\bar{\delta}_r$
0.1	0.35	−0.233	−0.171
0.25	0.35	−0.039	−0.072
0.5	0.35	0.005	0.025
0.75	0.35	0.003	0.019
1	0.35	0.012	0.086
1.5	0.35	0.018	0.201
0.1	0.59	−0.398	−0.217
0.25	0.59	−0.074	−0.102
0.5	0.59	0.017	0.067
0.75	0.59	0.018	0.073
1	0.59	0.017	0.099
1.5	0.59	0.018	0.151

The mean of the differences between the experimental and calculated values of t_r was evaluated from the values obtained for dextrans with different M_r.

4.3. Empirical equation for prediction of dispersion

As has been presented above, no known equation could reliably predict the variance of dextran solutes in our system. For that reason, we suggested an empirical equation that was used to fit the experimental data of dextran variance. The empirical equation was designed on the basis of the Taylor equation (Eq. (6)) that was rearranged into the following form,

$$ReSc = 96\frac{\sigma^2}{t_r^2}\frac{L_t}{d_t} \tag{20}$$

The equation was then proposed in a form of the following power function,

$$\frac{t_r^2}{\sigma^2} = a\frac{L_t}{d_t}Re^b Sc^c \tag{21}$$

which is typical for the correlation of the axial Péclet number in different systems. In order to account for the described effect of natural convection at short residence times, the dextran concentration of 1% was taken for the evaluation of the quantities used in Eq. (21).

The estimation of the parameters of Eq. (21) was performed independently for each short measuring tube when the data for different flow-rates and dextran molecular weights were fitted simultaneously. The estimated parameters and their 95% confidence intervals are given in Table 3. The mean relative error of t_r^2/σ^2 varied in the individual series from 14.5 to 24.2%. Obviously, these accuracies are not excellent but they are well compensated by the simplicity of the correlation for a broad range of solute sizes when the concentration effect on the solute viscosities and diffusivities could not be considered in such a simple equation. Figs. 7 and 8 illustrate the quality of the approximation of the experimental data using Eq. (21). Fig. 8 contains also the data for the KNO_3 dispersion that were obtained in a different chromatographic system and therefore they were not considered in fitting. It is evident that the extrapolation over one order of magnitude of the Schmidt numbers provided a quite good correspondence between the dispersion of high- and low-molecular solutes in the short tubes, respectively.

Table 3 shows that the highest accuracy of estimation was achieved at the exponent c which defines the curvature of the relationship of t_r^2/σ^2 versus Sc at a constant Re. It is significant that the value of c at all three tubes was rather close to −0.3. This result is in a good agreement with the value of an exponent of the relationship of the width of

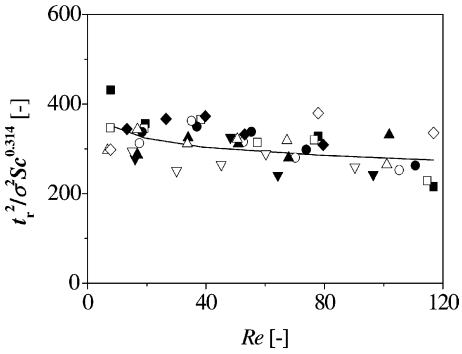

Fig. 7. Effect of the Reynolds number on dextran dispersion in a system with $L_t = 1.28$ m and $d_t = 0.25\times10^{-3}$ m. The symbols represent different relative molecular weights of dextrans: (■) 6000; (□) 9300; (●) 17,500; (○) 40,000; (▲) 60,000; (△) 70,000; (▼) 110,000; (▽) 200,000; (◆) 500,000; (◇) 2×10^6. The solid line represents the fit of the data with Eq. (21) using the parameter values from Table 3.

response in regard to diffusion coefficient equal to −0.36 that was achieved by Vanderslice et al. [36].

The higher error of the parameter b follows from that it was very close to 0. The minimum influence of the Reynolds number on t_r^2/σ^2, which is more clearly demonstrated in Fig. 7, means that the change of the flow rate (mean residence time) had a negligible influence on the relative spread of injected solute. This was probably the consequence of

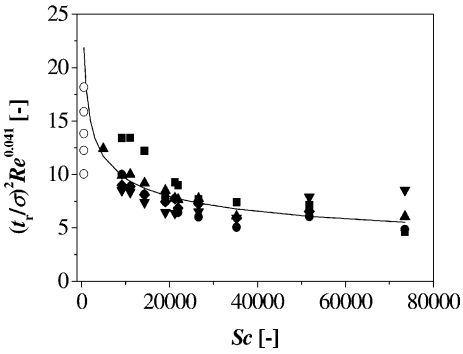

Fig. 8. Effect of the Schmidt number on dextran dispersion in a system with $L_t = 0.35$ m and $d_t = 0.5\times10^{-3}$ m. The symbols represent different flow rates: (■) 0.1 ml min^{-1}, (●) 0.25 ml min^{-1}, (▲) 0.5 ml min^{-1}, (▼) 0.75 ml min^{-1}, and (◆) 1 ml min^{-1}. The solid line represents the fit of the data with Eq. (21) using the parameter values from Table 3. For comparison, the data for the dispersion of KNO_3 at the flow rate of 0.5 ml min^{-1} in a different chromatographic system (The conditions are in the legend to Fig. 3) are given (○).

Table 3
Ninty-five percent confidence intervals of parameters of Eq. (21) for three different measuring tubes

L_t/d_t	V_t/V_s	a	b	c	δ_r
700	0.504	0.179 ± 0.170	−0.041 ± 0.063	−0.279 ± 0.009	0.200
1180	0.631	0.203 ± 0.246	$6\times10^{-4}\pm8\times10^{-4}$	−0.361 ± 0.111	0.242
5120	0.482	0.083 ± 0.065	−0.090 ± 0.052	−0.314 ± 0.074	0.145

V_t/V_s is the ratio of the volumes of measuring tube and system. The last column gives the mean relative error of the fitted quantity, t_r^2/σ^2.

the combined effect of convective dispersion and natural convection.

The smaller accuracy of the parameter a is a consequence of two factors. Firstly, it is the correlation with the exponent c where a small change in c invokes a large change in a. Secondly, a is basically an extrapolated value for $Re = 1$ and $Sc = 1$. Since our Schmidt numbers were far away from 1, the accuracy of the estimate of a had to be affected. It is interesting that the first two values of a in Table 3 are quite close especially when the uncertainties of their estimates and different fractions of the system volumes of these two tubes are considered. The third tube differed from the first two ones in that it had only a half diameter. The value of the parameter a was also approximately only half which means that the relative spread of the injected solute was larger in the narrower tube. At the same flow rates, the mean residence time in the narrower tube was about the same as that of the first tube from Table 3. It means that the value of τ (Eq. (4)) in the tube with half diameter was about four times larger. This implies that a stronger influence of axial dispersion and lower impact of natural convection could be expected in the narrower tube.

4.4. Dispersion in coiled tubes

The effect of tube coiling on solute dispersion was investigated using the single solute, dextran with $M_r = 70{,}000$. The measuring tubes with the length of 2 and 4 m were coiled into the circles with the radius of 5 and 6 cm, respectively. As has been explained in the Introduction and Theory, the tube coiling invokes centrifugal forces that cause secondary flow, which may result in a significant decrease of solute dispersion compared to the flow in a straight tube. The experimental values of the variances at different flow rates in both tubes are plotted in Fig. 9. Although the dimensionless times were here naturally higher than in the case of short, straight tubes, they were still smaller than 1. A fully developed axially dispersed flow was achieved neither in these cases although the tube length-to-diameter ratio reached a value of 8000.

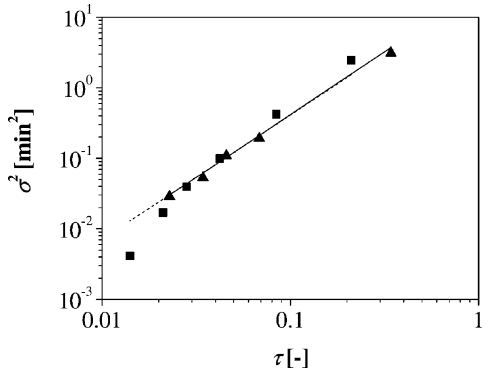

Fig. 9. Dispersion of dextran with $M_r = 70{,}000$ in coiled tubes with $d_t = 0.5 \times 10^{-3}$ m. The symbols belong to different tube lengths—(■) ($L_t = 2$ m), (▲) ($L_t = 4$ m). The lines represent the values of the variance calculated as the product of the ratio ϕ (Eq. (15)) and the variance in straight tube (Eq. (13))—dashed line ($L_t = 2$ m), solid line ($L_t = 4$ m).

A calculation procedure of the variance was based on a simple equation of Leclerc et al. (Eq. (11)) [47] that expresses the ratio of the variances in the coiled and straight tubes as a simple inverse third root function of the Reynolds number. Since Re varied in these experiments from about 4 to 64, the corresponding values of the ϕ-ratio were approximately in the interval from 0.46 to 0.19. As the tubes were too short for that the Taylor equation could be used to calculate the solute variance in the straight tube, the Kolev equation (Eq. (9)) was applied for that purpose. Multiplying this value with the corresponding ϕ-value, the variance in coiled tube was obtained. The calculated values of this variance are plotted in Fig. 9. The differences in the variances at the same dimensionless times for the two tube lengths were about 20–30% but their lines almost overlap in the scale used in Fig. 9. Obviously, a very good coincidence between the experimental and calculated variances was found except for one experiment, at the largest flow rate. This discrepancy could again be caused by the effect of natural convection.

5. Conclusions

The dispersion of macromolecular solutes with a broad range of molecular weights in the connecting tubes of standard chromatographic equipment has been the main objective of this paper. The set of dextrans was chosen as they are used as calibration standards in aqueous-phase size-exclusion chromatography. The implications of this work may, of course, be significant for other types of laboratory-scale chromatography employing high-molecular compounds as well.

At dextrans, the deviation from the axial dispersion model strongly increased with the molecular weight and flow rate when the experimental variance was up to thousand times smaller than the value calculated from the Taylor equation. The measured concentration signals had irregular shapes, typical for the early phases of the development of concentration profile after the pulse injection. The elimination of radial concentration profiles, which is characteristic for the axial dispersion flow, occurred in conventional chromatographic equipment only at KNO_3.

The experimental variances of dextrans, in general, did not comply with the equations designed for short tubes either. The most probable explanation for this discrepancy was the effect of natural convection that was caused by the density difference, albeit rather small one, between the injected solution and water. In spite of that the density difference was about the same at all dextrans, the residence time distributions differed significantly at the same conditions. This was an outcome of the interplay of natural convection, radial diffusion, and axial forced convection that was strongly affected by the values of diffusivities and viscosities, which depended on the molecular weight and concentration of dextrans.

A strong concentration dependence of the diffusivities and viscosities was a considerable complication for a good prediction of the dispersion of high-molecular solutes. Using the values of the initial concentration in the injected pulse, a relatively simple equation was designed that provided quite a good prediction of the variance of dextran concentration distribution at a specified configuration of the chromatographic system. It was found that the normalized variance, related to the squared mean residence time, depended mainly on the transport properties of the dextran solutions and only to lesser extent on the flow properties.

Besides the connecting tubing, other significant sources of extra-column dispersion were the thermostatted detector tube and in some experiments to lesser extent also the injection loop. An exact deconvolution of the experimental variance of concentration signal was however not the subject of investigation. It would be anyway difficult to achieve it without CFD simulations incorporating the momentum and mass balances for the connected parts of the chromatographic system.

Some experiments were made also at longer tubes that were coiled into a circle of a relatively low diameter. The theory predicts an existence of secondary centrifugal flow that results in a significant decrease of the variance of dispersed solute. The variance can be predicted as a product of a dimensionless parameter, which is the function of the Reynolds, Dean, and Schmidt numbers, and of the variance in a straight tube of the same length. Although previous applications of this approach were reported only for low-molecular solutes and long tubes where the Taylor equation could be applied, a very good coincidence with the experimental data was achieved in this case using the Kolev equation for the dispersion in short tubes. This implies that the bends and curvatures of chromatography tubing can result in a further significant decrease of dispersion of macromolecular solutes.

Acknowledgements

This work was supported by The Slovak Grant Agency for Science VEGA (Grant No. 1/0065/03).

Nomenclature

a, b, c	parameters of Eq. (21)
c_s	solute concentration (g dm^{-3})
d	tube diameter (m)
d_t	measuring tube diameter (m)
De	Dean number, Eq. (10)
D_0	diffusion coefficient at the infinite dilution (m^2 s^{-1})
D	diffusion coefficient (m^2 s^{-1})
D_L	dispersion coefficient (m^2 s^{-1})
$E(t)$	residence time distribution function
F	flow rate (ml min^{-1})
k_1, k_2	parameters of Eq. (14)
k_D	parameter of Eq. (15) (dm^3 g^{-1})
L	tube length (m)
L_t	measuring tube length (m)
M_r	relative molecular weight
n	number of theoretical plates
n_a	apparent number of theoretical plates, Eq. (8)
Pe	axial Péclet number (uL/D_L)
r	radial co-ordinate (m)
R	measuring tube radius (m)
Re	Reynolds number ($du\rho/\mu$)
S	detector signal
Sc	Schmidt number ($\mu/\rho D$)
t	time (min)
t_r	the mean residence time (min)
$t_{r,i}$	the mean residence time in injection loop (min)
u	mean flow velocity (m s^{-1})
u_0	tube axis flow velocity (m s^{-1})
V_i	injected volume (m^3)
V_s	volume of the chromatographic system (m^3)
V_t	volume of measuring tube (m^3)
x	axial co-ordinate (m)

Greek letters

$\bar{\delta}$, $\bar{\delta}_r$	absolute and relative errors
ϕ	ratio of diameters of tube and coil
$[\eta]$	intrinsic viscosity (cm^{-3} g^{-1})
φ	ratio of variances in coiled and straight tubes
μ	dynamic viscosity (Pa s)
μ_w	dynamic viscosity of water (Pa s)
ρ	density (kg m^{-3})
σ^2	variance (min^2)
σ_i^2	variance in injection loop, Eq. (19) (min^2)
σ_T^2	variance calculated from Eq. (6) (min^2)
τ	dimensionless time, Eq. (4)

References

[1] J.R. Conder, C.L. Young, in: Physicochemical Measurement by Gas Chromatography, Wiley, Chichester, 1978, p. 57.
[2] G.G. Dorsey, J.P. Foley, W.T. Cooper, R.A. Barford, H.G. Barth, Anal. Chem. 62 (1990) 324R.
[3] S.D. Kolev, Anal. Chim. Acta 308 (1995) 36.
[4] C.A. Lucy, L.L.M. Glavina, F.F. Cantwell, J. Chem. Educ. 72 (1995) 367.
[5] J.W. Dolan, LC-GC Int. 9 (1996) 530.
[6] J.W. Dolan, LC-GC Int. 11 (1998) 199.
[7] L.R. Snyder, J. Chromatogr. 125 (1976) 287.
[8] J.J. Kirkland, W.W. Yau, H.J. Stoklosa, C.H.J. Dilks, J. Chromatogr. Sci. 15 (1977) 303.
[9] C.E. Reese, P.R.W. Scott, J. Chromatogr. Sci. 18 (1980) 479.
[10] W. Kutner, J. Debowski, W. Kemula, J. Chromatogr. 218 (1981) 45.

[11] D.E. Games, M.J. Hewlins, D.J. Morgan, S.A. Westwood, J. Chromatogr. 250 (1982) 62.
[12] W.T. Kok, U.A.Th. Brinkman, R.W. Frei, H.B. Hanekamp, J. Chromatogr. 237 (1982) 357.
[13] R.P.W. Scott, C.F. Simpson, J. Chromatogr. Sci. 20 (1982) 62.
[14] K. Slais, D. Kourilova, J. Chromatogr. 258 (1983) 57.
[15] V. Kahle, M. Krejčí, J. Chromatogr. 321 (1985) 69.
[16] K.A. Cohen, J.D. Stuart, J. Chromatogr. Sci. 25 (1987) 381.
[17] O. Kaltenbrunner, A. Jungbauer, S. Yamamoto, J. Chromatogr. A 760 (1997) 41.
[18] R. Hahn, A. Jungbauer, Anal. Chem. 72 (2000) 4853.
[19] G. Taylor, Proc. R. Soc. Lond. A A219 (1953) 186.
[20] G. Taylor, Proc. R. Soc. Lond. A A223 (1954) 446.
[21] R. Aris, Proc. R. Soc. Lond. A A235 (1956) 67.
[22] G. Taylor, Proc. R. Soc. Lond. A A225 (1954) 473.
[23] V. Ananthakrishnan, W.N. Gill, A.J. Barduhn, AIChE J. 11 (1965) 1063.
[24] M.J.E. Golay, J.G. Atwood, J. Chromatogr. 186 (1979) 353.
[25] O. Levenspiel, W.K. Smith, Chem. Eng. Sci. 6 (1957) 227.
[26] J.F.K. Huber, A. Rizzi, J. Chromatogr. 384 (1987) 337.
[27] G. Liu, L. Svenson, N. Djordjevic, F. Erni, J. Chromatogr. 633 (1993) 25.
[28] J.P. Busnel, F. Foucault, L. Denis, W. Lee, T. Chang, J. Chromatogr. A 930 (2001) 61.
[29] W.N. Gill, Proc. R. Soc. Lond. A A298 (1967) 335.
[30] W.N. Gill, R. Sankarasubramanian, Proc. R. Soc. Lond. A A316 (1970) 341.
[31] J. Atwood, G.M.J.E. Golay, J. Chromatogr. 218 (1981) 97.
[32] A. Shankar, A.M. Lenhoff, AIChE J. 35 (1989) 2048.
[33] A. Shankar, A.M. Lenhoff, J. Chromatogr. 356 (1991) 235.
[34] E.B. van Akker, M. Bos, W.E. van der Linden, Anal. Chim. Acta 373 (1998) 227.
[35] J.S. Vrentas, C.M. Vrentas, Chem. Eng. Sci. 55 (2000) 849.
[36] J.T. Vanderslice, D.J. Higgs, A.G. Rosenfeld, K.K. Stewart, Talanta 28 (1981) 11.
[37] W.N. Gill, V. Ananthakrishnan, AIChE J. 13 (1967) 801.
[38] A. Bournia, J. Coull, G. Houghton, Proc. R. Soc. Lond. A A261 (1961) 227.
[39] N.S. Reejhsinghani, W.N. Gill, A.J. Garduhn, AIChE J. 12 (1966) 916.
[40] M. Vartuli, J.P. Hulin, G. Daccord, AIChE J. 41 (1995) 1622.
[41] L.A.M. Janssen, Chem. Eng. Sci. 31 (1976) 215.
[42] H. Soeberg, Chem. Eng. Sci. 43 (1988) 855.
[43] A.C. Ouano, J.A. Biesenberger, J. Chromatogr. 55 (1971) 145.
[44] Y. Vander Heyden, S.-T. Popovici, B.B.P. Staal, P.J. Schoenmakers, J. Chromatogr. A 986 (2003) 1.
[45] O. Levenspiel, Chemical Reaction Engineering, Wiley, New York, 1972.
[46] G. Guiochon, S.G. Shirazi, A.M. Katti, Fundamentals of Preparative and Nonlinear Chromatography, Academic Press, Boston, 1994.
[47] D.F. Leclerc, P.A. Bloxham, J. Toren, E. Clifford, Anal. Chim. Acta 184 (1986) 173.
[48] N.S. Pujar, A.L. Zydney, J. Chromatogr. A 796 (1998) 229.
[49] E. Nordmeier, J. Phys. Chem. 97 (1993) 5770.
[50] L. Lebrun, G.A. Junter, J. Membr. Sci. 88 (1994) 253.
[51] R. Hanselmann, W. Burchard, R. Lemmes, D. Schwengers, Macromol. Chem. Phys. 196 (1995) 2259.
[52] T.C. Laurent, L.O. Sundelof, K.O. Wik, B. Warmegard, Eur. J. Biochem. 68 (1976) 95.
[53] L. Lebrun, G.A. Junter, Enzyme Microb. Technol. 15 (1993) 1057.
[54] C. Wu, Macromolecules 26 (1993) 3821.
[55] M. Gille, E. Staude, Biotechnol. Bioeng. 44 (1994) 557.
[56] T.F. Kosar, R.J. Phillips, AIChE J. 41 (1995) 701.
[57] J. Paris, P. Guichardon, F. Charbit, J. Membr. Sci. 207 (2002) 43.
[58] D.R. Lide (Ed.), CRC Handbook of Chemistry and Physics, CRC Press, Boca Raton, 1992.